CHEMISTRY
A EUROPEAN JOURNAL

DOI: 10.1002/chem.201001438

Synthesis and Structural Aspects of *N*-Triflylphosphoramides and Their Calcium Salts—Highly Acidic and Effective Brønsted Acids

Magnus Rueping,* Boris J. Nachtsheim, René M. Koenigs, and Winai Ieawsuwan[a]

Abstract: Recently, 1,1′-bi-2-naphthol (BINOL)-based *N*-triflylphosphoramides emerged as a new class of potent Brønsted acid catalysts. In this paper we describe the efficient synthesis of various BINOL-based *N*-triflylphosphoramides and their calcium salts. Furthermore, X-ray crystal structure analysis combined with energy-dispersive X-ray spectroscopy (EDX) measurements confirmed that the synthesised chiral *N*-triflylphosphoramides are highly acidic metal-free catalysts.

Keywords: asymmetric synthesis · Brønsted acids · calcium · homogeneous catalysis · reaction mechanisms

Introduction

Recently, 1,1′-bi-2-naphthol (BINOL)-derived *N*-triflylphosphoramides emerged as a new class of highly acidic Brønsted acid catalysts. The application of the related chiral BINOL-derived phosphates in organocatalysis was first described in 2004 by the groups of Akiyama and Terada.[1] Since then, much effort has been devoted to the modification of the BINOL framework to obtain improved catalyst performance. Consequently, high levels of enantioselectivity were attained in various transformations.[2,3] However, due to their mild pK_a values (1–2),[4] BINOL-based phosphates are mainly restricted to the activation of basic aldimine and ketimine substrates. To lower their pK_a values and thus broaden the scope of substrate activation, the introduction of strong electron-withdrawing groups at the phosphate scaffold is required. In this context, it is well known that introduction of a triflate functionality into potential acidic groups leads to a substantial increase in the acidity.[5,6] For example, the monotriflylamide **1** has a pK_a value of 11.06, which implies nine orders of magnitude higher acidity than benzoic acid itself (pK_a = 20.7). An additional *N*-triflate moiety lowers the pK_a value to 6.17 (Scheme 1). The same behaviour has been observed for *p*-toluenesulfonamide. Here, the introduction of a triflate functionality decreases the pK_a value more than eight units from 16.3 to 8.0. By introducing a second triflate group, the pK_a value further decreases to 3.3 (Scheme 1).

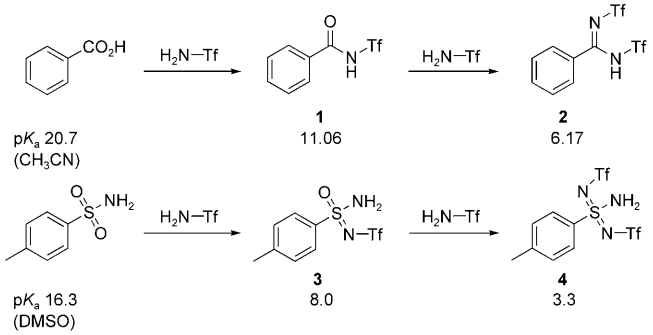

Scheme 1. Influence of trifluorphosphoramide substitution on the acidity of a protic acid.

Application of this concept to BINOL phosphates should lead to the corresponding BINOL-derived *N*-triflylphosphoramides with an estimated pK_a value of around −3 to −4. This represents a range in which carbonyl activation is feasible.

In 2006 Yamamoto and co-workers reported the first BINOL-based *N*-triflylphosphoramides and their application

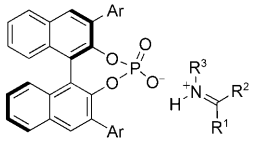

BINOL phosphate

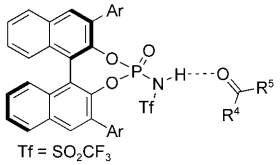

BINOL-*N*-triflylphosphoramide

[a] Prof. Dr. M. Rueping, Dr. B. J. Nachtsheim, Dipl.-Chem. R. M. Koenigs, Dr. W. Ieawsuwan
RWTH Aachen University, Institute of Organic Chemistry
Landoltweg 1, 52074 Aachen (Germany)
Fax: (+49)-241-809-2665
E-mail: magnus.rueping@rwth-aachen.de

in the asymmetric Diels–Alder reaction between ethyl vinyl ketone (**5**) and various siloxydienes **6** (Scheme 2a).[7] While

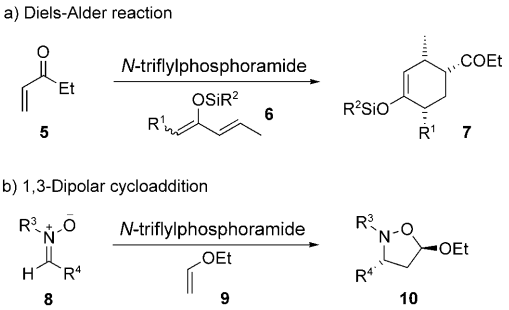

Scheme 2. *N*-Triflylphosphoramide-catalysed reactions developed by Yamamoto and co-workers.[7]

BINOL-phosphates showed no catalytic activity, the corresponding *N*-triflylphosphoramides efficiently catalysed this transformation. Accordingly, the desired cyclohexenes **7** were isolated in moderate to high yields and good enantioselectivities. Subsequently, *N*-triflylphosphoramides were applied in the 1,3-dipolar cycloaddition of nitrones **8** with ethyl vinyl ether (**9**) leading to products **10** with good to high diastereo- and enantioselectivities (Scheme 2b).[8]

Our group also developed several *N*-triflylphosphoramide-catalysed enantioselective reactions: 1) Nazarov cyclisations of divinylketones **11**,[9] 2) asymmetric 1,4-addition of indols **14** to β,γ -unsaturated α-ketoesters **13**[10] and 3) asymmetric ene reaction between styrenes **17** and trifluoromethylpyruvates **16** (Scheme 3a–c).[11] In contrast to BINOL phosphates, which exhibited low or no reactivity, the corresponding BINOL and H_8-BINOL-based *N*-triflylphosphoramides were highly effective in all of these transformations. Furthermore, with the aid of phosphoramides, we recently succeeded in the enantioselective synthesis of aminobenzopyrans **21**[12] and γ,γ′-disubstituted γ-lactams **24** via the formation of intermediary *N*-acyl iminium ions (Scheme 3d, e).[13]

So far, despite an increasing number of applications in asymmetric synthesis,[7–14] no systematic study for the efficient synthesis and structural determination of *N*-triflylphosphoramides and their calcium complexes was reported. This article not only aims to present an efficient route toward the synthesis of metal-free *N*-triflylphosphoramides, but for the first time provides mechanistic and structural insight into triflylphosphoramides as well as their calcium salts. Additionally, it provides evidence that the metal-free triflylphosphoramides are the active catalysts in diverse carbonyl reactions whereby specific acid catalysis activation is taking place.

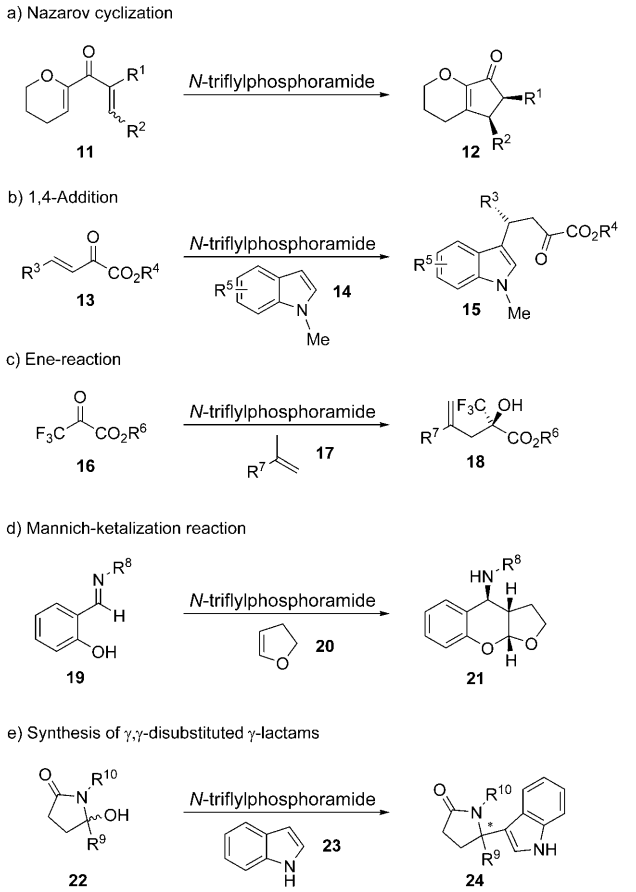

Scheme 3. *N*-Triflylphosphoramide-catalysed reactions developed by our group.

Results and Discussion

BINOL-*N*-triflylphosphoramides—Readily accessible highly acidic Brønsted acids: Although efficiently used in various asymmetric transformations, BINOL-derived *N*-triflylphosphoramides exhibit the same drawbacks as their phosphoric acid analogues, namely, their long synthesis. Nevertheless, different approaches towards the synthesis of 3,3′-aryl disubstituted BINOL derivative **29**, a valuable intermediate in the synthesis of BINOL phosphoramides, are known in the literature.[15] Our synthetic route starts from BINOL (**25**) and was accomplished in five steps (Scheme 4). Methoxymethyl (MOM) protection of the hydroxyl groups in **25** afforded **26** in high yield (90%). Metalation with *n*BuLi and subsequent iodination reaction gave the 3,3′-dihalogenated BINOL derivative **27**. The reaction proved to be sluggish and gave the desired product in moderate yield (55%). A considerable amount of monohalogenated byproduct was observed in this reaction. Alternatively, bromination led to the corresponding 3,3′-dibrominated species in a similar yield. Suzuki coupling with different boronic acids in the presence of $[Pd(PPh_3)_4]$ and $Ba(OH)_2$ yielded **28a–g**, which were subsequently deprotected to give the 3,3′-arylated BINOLs **29a–g** in high yields.[16] The phosphoramidation step was performed by following a similar procedure to the one described by Yamamoto and co-workers.[7] Treatment of **29a–g** with phosphoroxychloride generated the appropriate BINOL-phosphoroxychlorides, which were quenched in situ

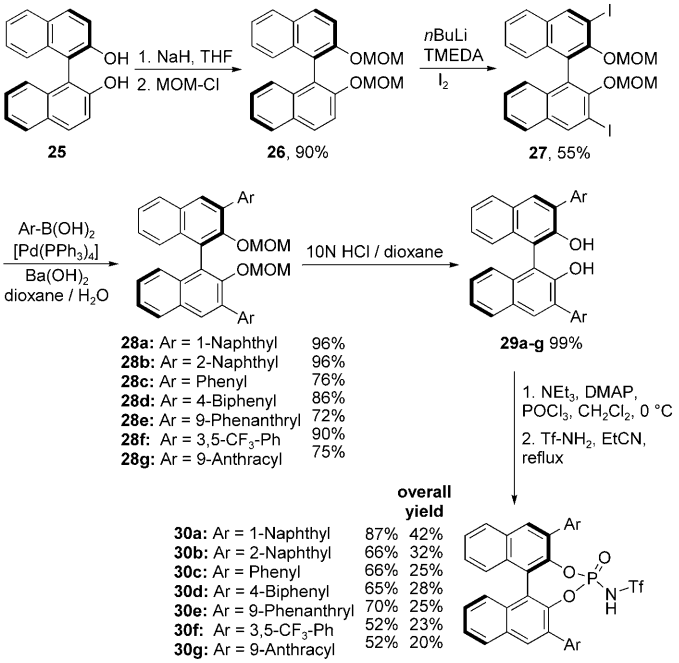

Scheme 4. Synthetic pathway to BINOL-*N*-triflylphosphoramides. TMEDA = N,N,N′,N′-tetramethylethylenediamine, DMAP = 4-dimethylaminopyridine, Tf = trifluoromethanesulfonyl.

with Tf-NH_2 to give the desired *N*-triflylphosphoramides **30a–g** in good to high yields (52–87%). The overall yields of this sequence vary between 20 and 42%, leaving space for further improvement (Scheme 4).

Synthesis of H_8-BINOL-*N*-triflylphosphoramides: To avoid the above-described drawbacks of the BINOL phosphoramide synthesis, our attention turned to a slightly different substance class, namely, the corresponding H_8-BINOL derivatives. For instance, an efficient procedure for the bromination of H_8-BINOL to 3,3′-dibromo-H_8-BINOL is known.[17] Furthermore, Beller and co-workers developed a very elegant methodology for the direct Suzuki coupling of unprotected H_8-BINOLs.[18] The combination of both leads to a procedure that circumvents the use of protecting groups as well as MOM-Cl and prevents the low yielding halogenation step of the above-described synthetic route (Scheme 4).

The synthesis starts with the hydrogenation of (*R*)-BINOL (**25**), which was performed at 80°C and 80 bar H_2 by using Pd/C (Scheme 5). The desired H_8-BINOL (**31**) was isolated in quantitative yield (99%) after 12 h. Bromination was accomplished at −30°C by adding bromine to **31** and the corresponding 3,3′-dibrominated derivative **32** was obtained in 91% yield after crystallisation. Compared with BINOL halogenation, the present reaction is much easier to achieve, especially when performed on larger scale. By using the protocol described by Beller and co-workers ($Pd(OAc)_2$, cataCXiumA (**33**) as phosphine ligand),[18] Suzuki coupling of **32** with different boronic acids could be directly performed, without the need for *O*-protection. The products **34a–i** were obtained in good to excellent yields (77–95%).

The final phosphoramidation step was carried out in a one-pot fashion by subsequently adding $POCl_3$ and Tf-NH_2 to a solution of the 3,3′-arylated H_8-BINOLs.

Compared with the synthesis of related BINOL *N*-triflylphosphoramides (Scheme 4), this process avoids the *O*-protection/deprotection steps and leads to H_8-*N*-triflylphosphoramides **35a–m** in excellent overall yields (52–85%).

Synthesis of H_8-3,3′-silylated *N*-triflylphosphoramides: For a greater diversity of the BINOL scaffold, we were interested in the synthesis of the corresponding 3,3′-silylated derivatives. Here, a highly efficient route to the corresponding diols **37** is known.[19]

The synthesis starts from the 3,3′-dibromo H_8-BINOL (**32**) and involves, in a first step, protection of the alcohol moieties with either $ClSiPh_3$ or $ClSiPh_2Me$ (Scheme 6). The *O*-protected BINOL derivatives **36a** and **36b** were treated with *t*BuLi to initiate a Brook-type rearrangement to the desired 3,3′-silylated H_8-BINOLs **37a** and **37b**. The phosphoramidation step was performed in the same manner as described above. Whereas the phosphoramidation of sterically high demanding 3,3′-$SiPh_3$ derivative **37b** was straightforward (67%), phosphoramidation of the 3,3′-$SiPh_2Me$-substituted derivative **37a** was accomplished in only 46% yield. The overall yields of this sequence are 57 and 34%, respectively.

Crystal structure analysis of the *N*-triflylphosphoramide calcium salts: In addition to the developed synthetic pathways, the elucidation of the *N*-triflyphosphoramides structure constituted another focus of interest. In particular, for their future design it is relevant to know whether the acidic proton is located at the sulfonamide nitrogen or at the phos-

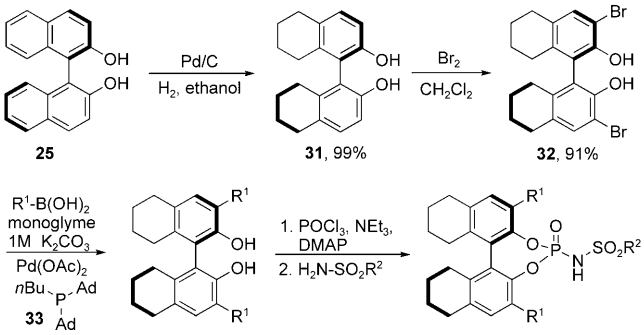

	R^1	
34a:	1-Naphthyl	83%
34b:	2-Naphthyl	91%
34c:	Phenyl	85%
34d:	4-Biphenyl	90%
34e:	9-Phenanthryl	82%
34f:	3,5-CF_3-Ph	95%
34g:	Mesityl	94%
34h:	PMP	77%
34i:	4-*t*Bu-Phenyl	95%

	R^1	R^2		overall yield
35a:	1-Naphthyl	CF_3	89%	67%
35b:	2-Naphthyl	CF_3	83%	68%
35c:	Phenyl	CF_3	97%	74%
35d:	4-Biphenyl	CF_3	90%	79%
35e:	9-Phenanthryl	CF_3	72%	53%
35f:	3,5-CF_3-Ph	CF_3	99%	85%
35g:	Mesityl	CF_3	75%	63%
35h:	PMP	CF_3	76%	53%
35i:	4-*t*Bu-Phenyl	CF_3	65%	56%
35j:	Phenyl	C_4F_9	94%	71%
35k:	Phenyl	C_8F_{17}	95%	73%
35l:	Phenyl	4-CF_3-Ph	67%	52%
35m:	Br	CF_3	74%	67%

Scheme 5. Efficient synthetic route to H_8-BINOL-*N*-triflylphosphoramides.

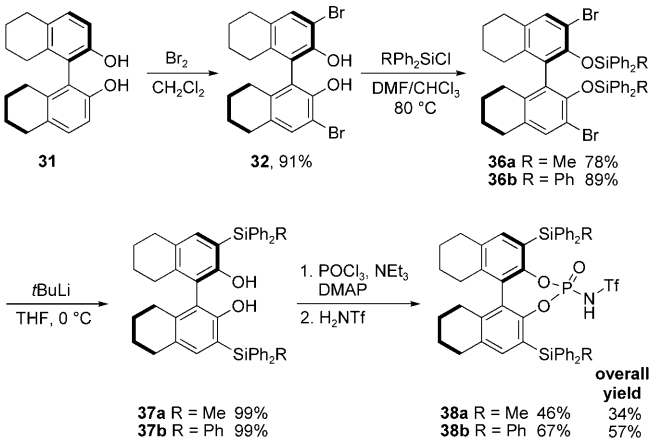

Scheme 6. Synthesis of 3,3′-silylated H_8-BINOL-*N*-triflylphosphoramides.

phate oxygen (Scheme 7). So far, only one crystal structure showing a deprotonated BINOL *N*-triflylphosphoramide was published.[8] Hence, we started our own crystallisation

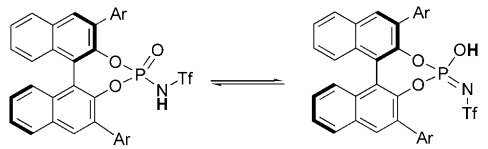

Scheme 7. Equilibrium between *N*-triflylphosphoramide and *N*-triflylphosphorimide.

experiments with various *N*-triflylphosphoramides. We were pleased to find that the structure of *p*-methoxyphenyl-substituted *N*-triflylphosphoramide **35h** could be examined by X-ray crystal structure analysis.

Surprisingly, we did not observe the expected free acid **35h**, but its corresponding calcium salt Ca(**35h**)$_2$ (Figure 1). At first sight this was intriguing, since no calcium derivatives were used during the synthesis or workup procedures. On the other hand, the structure of *N*-triflylphosphoramide resembles the structure of acetylacetonate. Therefore, similar chelating properties for cation binding can be envisioned (Figure 2).

Important bond lengths and angles of this structure are summarised in Table 1. The P1B–O3B bond length is 147.4 pm and therefore even shorter than a theoretical P=O double bond (152.0).[20] The S1B–O1SB bond with O1 coordinated to calcium is 144.1 pm and again shorter than a theoretical S=O double bond (150.0 pm). The non-coordinating S1B–O2SB bond length is 141.6 pm. Furthermore, the P1B–N1B (160.5 pm) and the S1B–N1B (152.9 pm) bond lengths are both significantly shorter than the corresponding theoretical bond length for a N–X single bond (180.0 and 174 pm, respectively),[20] thus indicating a double-bond character for the two bonds. The calcium ion possesses distorted pentagonal bipyramidal geometry with two phosphoramides and one water molecule in the equatorial plane. The axial sites are occupied by water and dioxane (Figure 1). The

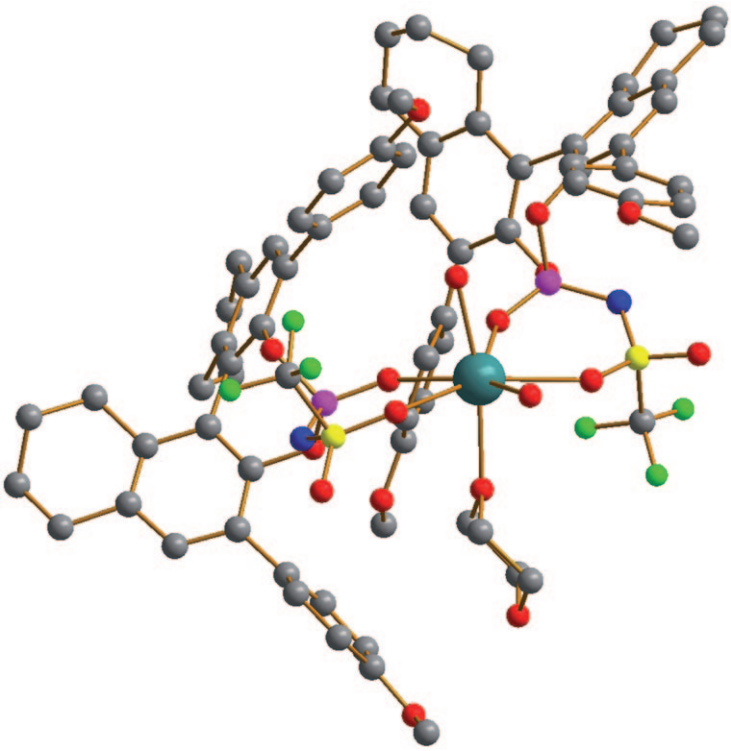

Figure 1. Crystal structure of Ca(**35h**)$_2$.

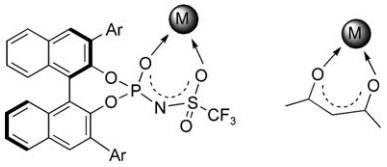

Figure 2. Chelating properties of *N*-triflylphosphoramides.

Ca1A–O3B and Ca1A–O1SB bond lengths are 236.9 and 245.2 pm, respectively.

Further crystals have been obtained for the 3,3′-(2-naphthyl)-disubstituted *N*-triflylphosphoramide **30b** (Figure 3). Once more, we did not observe the free acid, but its calcium salt Ca(**30b**)$_2$. As in the previous structure, the calcium ion is pentagonal bipyramidal surrounded by one water and two phosphoramide molecules in the pentagonal sites and two dioxane molecules in the axial sites.

Chiral ligands incorporating a sterically demanding H_8-binaphthyl moiety instead of the unsaturated analogue are known to give increased selectivity in several metal-based catalysed reactions.[21] The higher selectivity observed in these transformations is accounted for by the greater torsion angle of the H_8-binaphthyl scaffold. However, this seems not to be the case for the phosphoramide derivatives. A close look at the crystal structures of Ca(**35h**)$_2$ and Ca(**30b**)$_2$ reveals almost the same torsion angle for both partially saturated and unsaturated backbones. A slightly smaller torsion angle has been observed in the case of the unsaturated BINOL system.

Table 1. Selected bond lengths [pm] and angles [°] of Ca(**35h**)$_2$ and Ca(**30b**)$_2$ as obtained by X-ray diffraction. Coordination sphere of calcium in Ca(**35h**)$_2$ (*para*-methoxyphenyl residues and hydrogen atoms have been omitted for clarity).

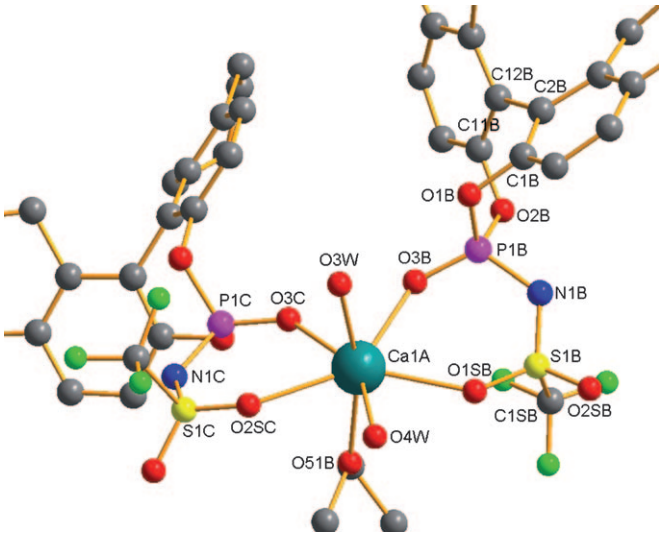

	Ca(**35h**)$_2$	Ca(**30b**)$_2$		Ca(**35h**)$_2$	Ca(**30b**)$_2$
P1B–O3B	147.4(6)	147.4(6)	Ca1A–O3B	236.9(6)	234.8(0)
P1B–N1B	160.5(7)	160.8(9)	O3B-P1B-N1B	118.7(3)	120.0(6)
P1B–O2B	161.1(5)	160.6(0)	P1B-N1B-S1B	123.7(4)	125.5(6)
P1B–O1B	158.6(5)	161.1(5)	Ca1A-O1SB-S1B	142.0(4)	142.4(9)
S1B–N1B	152.9(8)	153.7(4)	Ca1A-O3B-P1B	136.8(3)	140.0(9)
S1B–O1SB	144.1(7)	144.9(9)	O1SB-Ca1A-O3B	71.9(2)	73.5(7)
S1B–O2SB	141.6(7)	142.6(9)	N1B-S1B-C1SB	103.6(5)	103.3(1)
S1B–C1SB	182.(1)	182.4(8)	C1B-C2B-C12B-C11B	56.(1)	54.9(3)
Ca1A–O1SB	245.2(7)	245.8(1)			

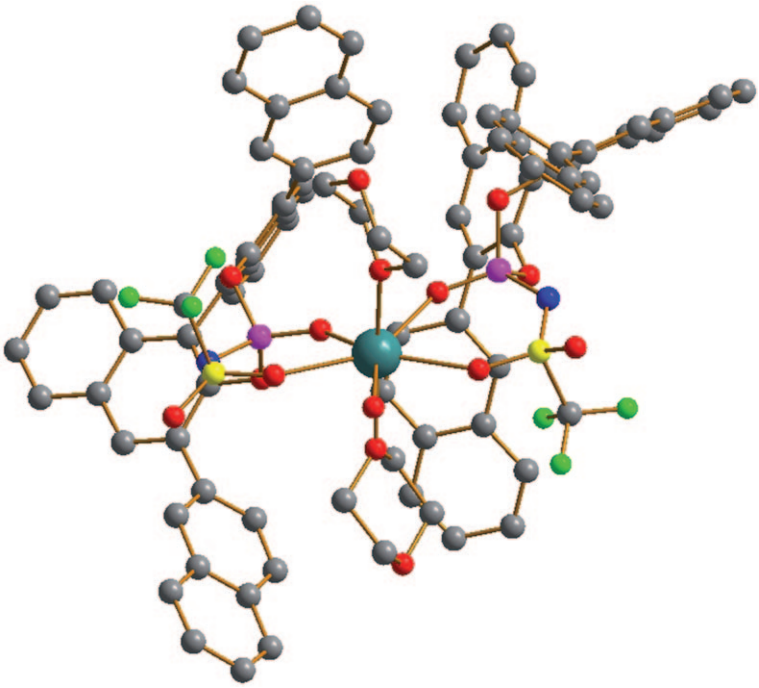

Figure 3. Crystal structure of Ca(**30b**)$_2$.

;Crystal structure analysis of the H$_8$-3,3′-*p*-methoxyphenyl (PMP)-substituted *N*-triflylphosphoramide 35h: The described calcium salts Ca(**30b**)$_2$ and Ca(**35h**)$_2$ were obtained after purification of **30b** and **35h** by column chromatography using commercially available silica gel containing traces of calcium. However, after a final washing with 5 N HCl, we always observed a change in the product consistency and colour. Therefore, different crystallisation experiments of *N*-triflylphosphoramides obtained after the final washing were initiated. Suitable single crystals for X-ray analysis have been obtained for catalyst **35h**. The molecular structure is shown in Figure 4. The asymmetric unit cell consists of two crystallographically independent molecules forming a dimeric structure. The *N*-triflyl functionalities of the two molecules in the dimeric structure are facing each other, building a polar pocket. The pocket is held together by two hydrogen bonds and is shielded on the reverse side by two *p*-methoxyphenyl moieties, one from each molecule. No metal ions are present in the crystal structure, demonstrating that the catalytically active species is indeed a protonated, highly acidic Brønsted acid. Furthermore, in the solid state, the proton is located at the nitrogen atom without any evidence for tautomerism between phosphoramide and phosphorimide.

The acidic proton is involved in a hydrogen bond with the Lewis basic P=O functionality of the second *N*-triflylphosphoramide within the asymmetric unit. Each molecule acts as a hydrogen-bond donor and acceptor. The values for the two corresponding hydrogen bonds are 201.80 and 182.76 pm, respectively (Table 2). The length

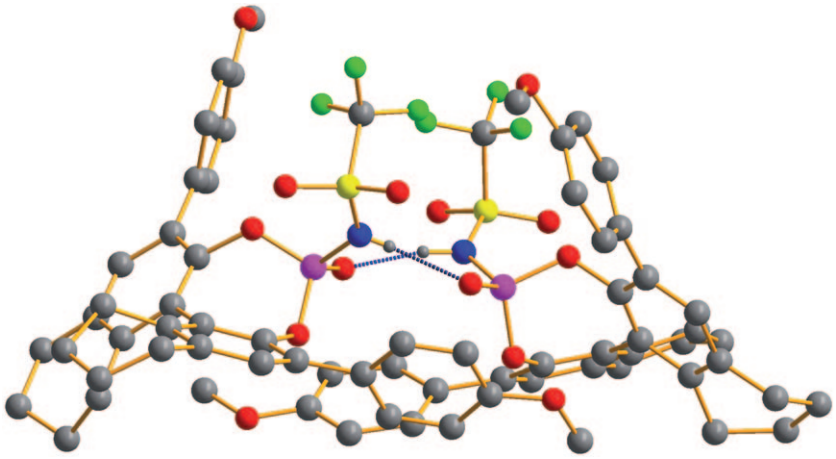

Figure 4. Crystal structure of the dimer of *N*-triflylphosphoramide **35h**.

of the P=O double bond (146 pm) in both molecules is similar to the length of the P=O double bond in the calcium salt and in the previously disclosed BINOL phosphates. This result suggests that dimer formation has no significant influence on the P=O double bond.

A comparison of the bond lengths in the structure of calcium salt Ca(**35h**)$_2$ (Table 1) and the corresponding free acid **35h** (Table 2) shows that both S–N and P–N bonds, are significantly longer for the protonated *N*-triflylphosphoramide. The S–N bond lengthens from 152.9 to 162.5 pm and the P–N bond from 160.5 to 167.1 pm. This is due to protonation, which disturbs the conjugation in the anion of the *N*-triflylphosphoramide. Nevertheless, S–N and P–N bonds are shorter than expected for the corresponding single bonds. None of the S–O bonds are involved in the chelation of a metal ion or proton; consequently they are all of almost identical length (142 pm).

Energy-dispersive X-ray spectroscopy (EDX) measurements of 35h: To confirm that the washing step removes putative metal impurities, such as calcium, EDX spectra of **35h** were analysed.

The diagrams displayed in Figure 5 show the EDX spectra of a sample before (top) and after (bottom) the final HCl washing procedure. As expected, in the upper spectra the K_α peaks for carbon, oxygen, fluorine, phosphor and sulfur at 0.28, 0.52, 0.67, 2.01 and 2.30 keV respectively can be observed. Furthermore, we notice calcium K_α and K_β peaks at 3.69 and 4.01 keV, respectively. The P/S/Ca ratio is 2:2:1, which is in agreement with the measured X-ray structure of the calcium salt Ca(**35h**)$_2$. Since no calcium ions are present during the synthetic steps, it is likely that *N*-triflylphosphoramides bound calcium cations from the silica gel used for the final column chromatography. Nevertheless, we were pleased to see that no calcium was detected in a sample obtained after twice extracting Ca(**35h**)$_2$ with 5 N HCl. In this context, BINOL phosphoric acids are known to bind calcium upon purification on silica gel and to release it upon acidic washing.[22] Regarding our analysed sample, no other heavy metal impurities, for example, Pd, Rh or Ru, have been found on a ppm level. Even with total X-ray reflection fluorescence (TXRF), a method much more sensitive than EDX, no heavy metals were detected in our samples. Therefore, we can conclude that the synthesised *N*-triflylphosphoramides do not contain any metal impurities and their activation mode is based on their highly acidic proton.

Table 2. Selected bond lengths [pm] and angles [°] of **35h** as obtained by X-ray diffraction. Close-up view of the two hydrogen bonds forming the polar cavity/dimer (*para*-methoxyphenyl residues and hydrogen atoms have been omitted for clarity).

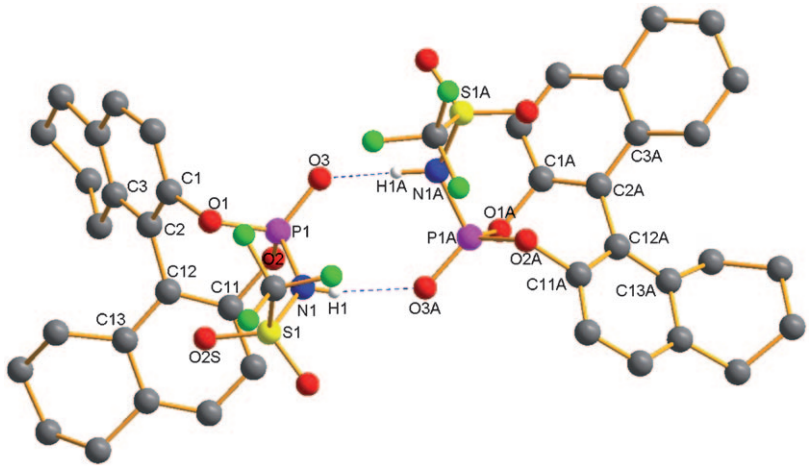

P1–O1	156.78/158.83(1)	H1A···O3	182.76
P1–O2	158.01(1)/157.03(1)	N1-H1-O3A	167.91
P1–O3	146.0(3)/146.3(1)	N1A-H1A-O3	169.54
P1–N1	167.6 (7)/167.1(1)	P1-O3-H1A	129.05
S1–N1	162.5(1)/161.1(1)	P1 A-O3A-H1	133.43
S1=O2S	141.92(1)	P1-N1-S1	133.80/132.07
H1···O3A	201.80	C11-C12-C2-C1	56.29/54.64

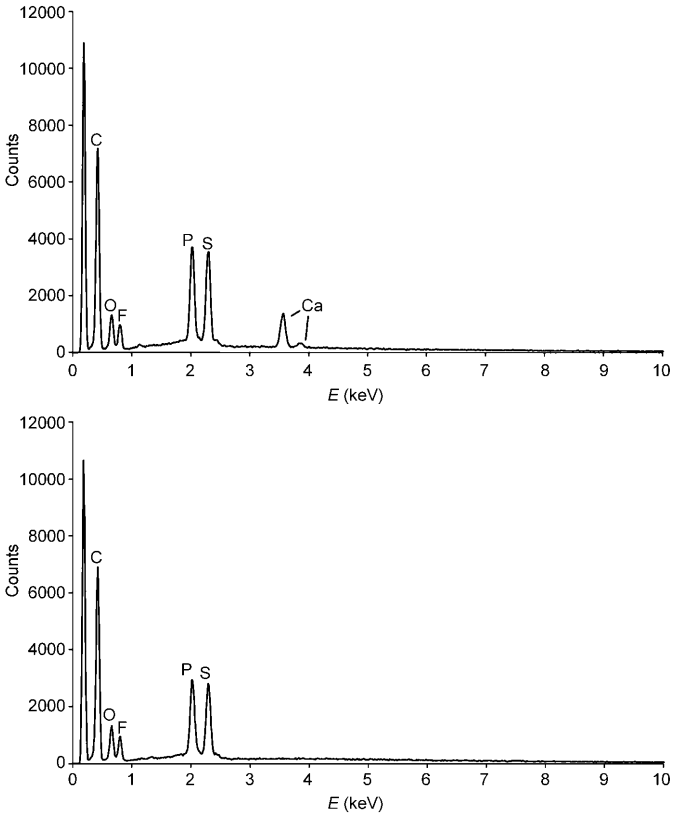

Figure 5. EDX spectra of H_8-*N*-triflylphosphoramide **35h** before (top) and after washing with 5 N HCl (bottom).

Kinetic studies of the *N*-triflylphosphoramide-catalysed ene reaction: In addition to revealing the structure and properties of this new class of highly acidic *N*-triflylphosphoramides, we were interested in finding out the kinetic laws these catalysts obey. The recently disclosed carbonyl ene reaction was chosen as a model for subsequent kinetic studies. Since the two components trifluoropyruvic ester (**16a**) and α-methylstyrene (**17a**) react in a clearly defined manner, the reaction can easily be followed by NMR spectroscopy. In addition, general reaction parameters, such as solvent, temperature and reaction time, are well suited for good resolved NMR spectra. Regarding the mechanism, we propose that upon activation of the trifluoropyruvic ester by the *N*-triflylphosphoramide, nucleophilic attack by the α-methylstyrene takes place, releasing the *N*-triflylphosphoramide **39** and forming the α-hydroxy-α-trifluoromethyl ethyl ester **18a**.

Depending on the relative reaction rates, the present catalysis reactions (Scheme 8) exhibit general or specific acid-catalysed kinetics. In the case of specific acid catalysis, k_1 is fast and the addition of the nucleophile to the active complex is the rate-determining step, thus one should observe reaction kinetics that are independent of the acid concentration. In the general acid-catalysed reaction, the acid is involved in the rate-determining step and its concentration influences the reaction rate.

First the background reaction was monitored by the consumption of pyruvic ethyl ester. We were pleased to see that

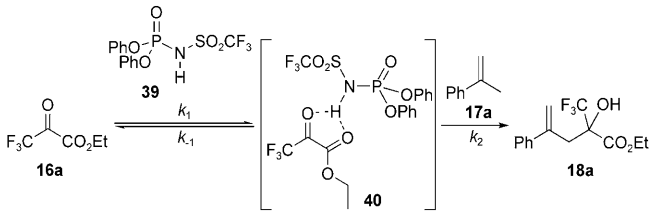

Scheme 8. Proposed reaction mechanism for the carbonyl ene reaction.

the background reaction takes place only slowly. In further experiments the same reaction was run with 1, 2, 5 and 10 mol% of the catalyst (Figure 6).

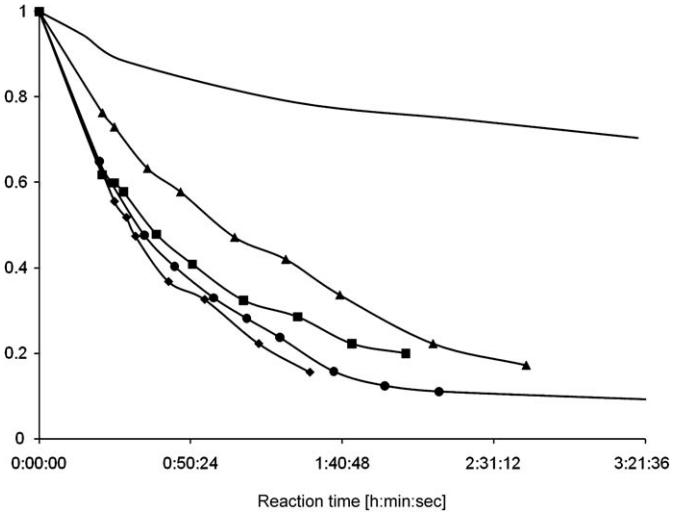

Figure 6. Reaction kinetics for the carbonyl ene reaction using different catalyst loadings. ——: background reaction, ◆: 1 mol%, ●: 2 mol%, ■: 5 mol% and ▲: 10 mol%.

The observed reaction kinetics (Figure 6) suggest that the effect of catalyst loading is only minimal. Reactions performed with 1, 2 and 5 mol% of catalyst proceeded with almost the same reaction constants. In contrast, the reaction carried out with 10 mol% of catalyst appeared to be significantly slower than the reactions performed with lower catalyst loadings. This result might be explained through a concentration effect: with increasing the concentration of the less demanding, achiral catalyst **39** (Scheme 8), catalyst dimerisation is favoured and consequently the catalytic activity drops. The similar reaction constants indicate that the concentration of the Brønsted acid has no effect on the reaction kinetics, meaning that a specific acid-catalysed reaction takes place. Thus the rate-determining step is the addition of the α-methylstyrene to the activated pyruvic ester.

Conclusion

We have established an efficient synthetic route which gives access to H_8-BINOL *N*-triflylphosphoramides. Crystal struc-

ture analysis and EDX measurements confirm that these highly acidic Brønsted acids are free from any metal impurities. Furthermore, kinetic studies of the *N*-triflylphosphoramide-catalysed ene reaction strongly indicates specific acid catalysis as the activation mode. These results support the theory that these Brønsted acids are strong enough to promote carbonyl activation. Acidity measurements as well as further NMR spectroscopy studies in solution are part of ongoing experiments and will be reported in due course.

Experimental Section

General: Unless otherwise noted, all commercially available compounds were used as provided by the suppliers. Solvents for chromatography were technical grade and distilled prior to use. Dichloromethane and propionitrile used in reactions were reagent grade and distilled from CaH_2. Analytical thin-layer chromatography (TLC) was performed on Merck silica gel aluminium plates with F-254 indicator, visualised by irradiation with UV light. Column chromatography was performed by using silica gel Merck 60 (particle size 0.063–0.2 mm). Solvent mixtures are reported as volume/volume ratios. ^{1}H and ^{13}C NMR spectra were recorded on a Bruker AM 250 spectrometer, a Bruker AV 300 and a Varian Inova 400 spectrometer in $CDCl_3$. Data are reported in the following order: chemical shift (δ) in ppm; multiplicities are indicated, s (singlet), d (doublet), t (triplet), m (multiplet); coupling constants (*J*) are in Hertz (Hz). Mass spectra (ESI-MS) were conducted on an ESI-MS: VG-Platform II (Fisons Instruments) spectrometer. Mass spectra (EI-MS, 70 eV) were conducted on GC-MS Shimadzu QP2010 (column: Equity-5, length × I.D. 30 m × 0.25 mm, df 0.25 μm, lot # 28089-U, Supelco) or Finnigan MAT SSQ 700 (MS-EI, 70 eV) instruments. IR spectra were recorded on a Jasco FT/IR-420 spectrometer and are reported in terms of frequency of absorption (cm^{-1}). Optical rotations were measured on a Perkin–Elmer 241 polarimeter.

Hydrogenation of 25 to form 31: (*R*)-BINOL (10 g, 35 mmol) and Pd/C (5 g, 5 wt% Pd/59.5 wt% H_2O) were suspended in ethanol (80 mL) and stirred for 20 h under 80 bar H_2 pressure at 90 °C in an autoclave. After the hydrogenation was finished, the crude suspension was filtered over Celite and subsequently over a short plug of silica gel to provide H_8-(*R*)-BINOL **31** as a white powder in quantitative yield (99%, 10.2 g). ^{1}H NMR (250 MHz, $CDCl_3$): $\delta = 7.11$ (d, $J = 8.3$ Hz, 2H), 6.87 (d, $J = 8.3$ Hz, 2H), 4.63 (s, 2H), 2.86–2.71 (m, 4H), 2.42–2.13 (m, 4H), 1.85–1.66 ppm (m, 8H); ^{13}C NMR (100 MHz, $CDCl_3$): $\delta = 151.4$, 137.2, 131.1, 130.2, 118.9, 113.0, 29.3, 27.2, 23.1, 23.0 ppm; EI-MS: *m*/*z* (%): 294.1 (100) $[M]^+$.

Bromination of 31 to form 32: Compound **31** (15 g, 51 mmol) was dissolved in dichloromethane (280 mL) and the solution was cooled to −30 °C. Br_2 (5.7 mL, 112 mmol) was then added. The reaction mixture was stirred for 30 min at −30 °C and subsequently treated with a saturated aqueous solution of $Na_2S_2O_5$ (250 mL). The suspension was warmed to RT and stirred for an additional 60 min. The organic layer was separated, the aqueous phase was washed twice with dichloromethane and the combined organic layer was washed again with a saturated aqueous solution of $NaHCO_3$, dried over Na_2SO_4, filtered and evaporated under vacuum to yield a yellow foam. The crude mixture was recrystallised from heptane to give **32** as colourless crystals (21.02 g, 91%). ^{1}H NMR (300 MHz, $CDCl_3$): $\delta = 7.31$ (s, 2H), 5.12 (s, 2H), 2.79 (t, 4H, $J = 4.2$ Hz), 2.35–2.27 (m, 2H), 2.17–2.08 (m, 2H), 1.78–1.66 ppm (m, 8H); ^{13}C NMR (100 MHz, $CDCl_3$): $\delta = 147.2$, 136.8, 132.6, 131.5, 122.2, 107.2 ppm; EI-MS: *m*/*z* (%): 371.0 (9) $[M-Br]^+$, 373.0 $[M-Br]^+$, 292.1 $[M-Br_2]^+$; ESI-MS: *m*/*z* (%): 449.1 (54) $[M-H]^-$, 451.1 (100) $[M-H]^-$, 453.0 (53) $[M-H]^-$.

Suzuki Coupling of 32 to form 34d: Compound **32** (4.1 g, 9 mmol) and 4-biphenyl boronic acid (5.4 g, 27 mmol) were suspended in a mixture of glycol ether (90 mL) and 1 M K_2CO_3 (45 mL). The suspension was repeatedly degassed and $Pd(OAc)_2$ (81 mg, 0.36 mmol, 4 mol%) and CataCXium A [$P(Ad)_2(Bu)$] (162 mg, 0.45 mmol, 5 mol%) were added under an argon atmosphere. The mixture was heated at reflux under an argon atmosphere for 24 h. The reaction mixture was cooled to RT, triturated with dichloromethane and the organic layer was separated. The aqueous phase was twice washed with dichloromethane. The combined organic layer was washed with a saturated aqueous solution of NH_4Cl and brine, dried over Na_2SO_4, filtered and evaporated under vacuum. The crude oil was purified by flash chromatography (silica gel, hexane to hexane/dichloromethane 2:1) to give a white powder (4.9 g, 8.2 mmol, 90%). ^{1}H NMR (250 MHz, $CDCl_3$): $\delta = 7.84$–7.69 (m, 12H), 7.58–7.49 (m, 4H), 7.46–7.38 (m, 2H), 7.30 (s, 2H), 5.04 (s, 2H), 2.95–2.86 (m, 4H), 2.59–2.46 (m, 2H), 2.44–2.29 (m, 2H), 1.94–1.76 ppm (m, 8H); ^{13}C NMR (100 MHz, $CDCl_3$): $\delta = 148.3$, 141.0, 139.9, 136.9, 136.8, 131.8, 130.4, 129.7, 128.8, 127.3, 127.2, 125.7, 120.1, 29.4, 27.3, 23.2, 23.1 ppm; ESI-MS: *m*/*z* (%): 597.7 (61) $[M-H]^-$.

Compound 34i: White foam; m.p. 128–130 °C; $[\alpha]_D^{20} = -66.5$ ($c = 0.5$, $CHCl_3$); ^{1}H NMR (400 MHz, $CDCl_3$): $\delta = 7.54$ (d, $J = 8.6$ Hz, 4H), 7.45 (d, $J = 8.6$ Hz, 2H), 7.16 (s, 2H), 4.93 (b, 2H), 2.75–2.85 (m, 4H), 2.35–2.45 (m, 2H), 2.24 (dt, $J = 17.4$ Hz, $J = 6.2$ Hz, 2H), 1.66–1.82 (m, 8H), 1.36 ppm (s, 18H); ^{13}C NMR (100 MHz, $CDCl_3$): $\delta = 149.8$, 148.0, 136.2, 134.8, 131.5, 130.0, 128.7, 125.7, 125.3, 120.0, 34.6, 31.4, 29.3, 27.2, 27.0, 23.2 ppm; IR (KBr): $\nu = 3518$, 2929, 2861, 2323, 2106, 1666, 1606, 1516, 1457, 1393, 1361, 1322, 1268, 1233, 1178, 1137, 1022, 945, 834 cm^{-1}; EI-MS: *m*/*z* (%): 558 (100) $[M]^+$, 543 (25), 264 (31).

Synthesis of 35a: Compound **34a** (1 g, 1.8 mmol) was dissolved in dry dichloromethane (15 mL) and cooled to 0 °C under argon atmosphere. Triethylamine (1.81 mL, 12.8 mmol, 7 equiv), $POCl_3$ (226 mg, 2.2 mmol, 1.2 equiv) and DMAP (447 mg, 3.7 mmol, 2 equiv) were added. The reaction mixture was stirred for 2 h at RT. Tf-NH_2 (681 mg, 4.6 mmol, 2.5 equiv)and dry propionitrile (8 mL) were added and the reaction mixture was heated at reflux at 85 °C for 4 h. The solution was cooled to RT, quenched with water and stirred for 1 h. The solution was extracted three times with diethyl ether, the organic layers were combined, washed once with a saturated aqueous solution of $NaHCO_3$, twice with 5 N HCl, dried over Na_2SO_4, filtered and evaporated under vacuum. The crude product (yellow oil) was purified by flash chromatography (hexane/dichloromethane/diethyl ether 1:1:0.5) to yield a white solid. This solid was dissolved in dichloromethane and washed again twice with 5 N HCl to yield **35a** as a white foam (1.2 g, 89%). M.p. 254–258 °C; $[\alpha]_D^{20} = -221.2$ ($c = 0.5$, $CHCl_3$); ^{1}H NMR (300 MHz, $CDCl_3$): $\delta = 7.92$–7.63 (m, 4H), 7.62–7.32 (m, 8H), 7.32–7.03 (m, 4H), 5.04 (brs, 1H), 3.00–2.79 (m, 5H), 2.61–2.44 (m, 2H), 2.19–2.04 (m, 1H), 2.03–1.67 ppm (m, 8H); ^{13}C NMR (100 MHz, $CDCl_3$): $\delta = 133.2$, 133.1, 132.4, 131.9, 131.7, 128.2, 128.1, 128.0, 127.9, 126.0, 126.0, 125.9, 125.8, 125.8, 125.5, 125.5, 124.9, 44.9, 29.3, 29.3, 28.1, 28.0, 22.7, 22.6, 22.59 ppm; ^{19}F NMR (282 MHz, $CDCl_3$) : $\delta = -78.70$ ppm; ^{31}P NMR (121 MHz, $CDCl_3$): $\delta = -3.01$ ppm; IR (KBr): $\nu = 3442$ (b), 2932, 1294, 1197, 1088, 956, 892, 779, 607 cm^{-1}; ESI-MS: *m*/*z* (%): 738.7 (100) $[M-H]^-$.

Compound 35b: White foam; m.p. 200–203 °C; $[\alpha]_D^{20} = -284.0$ ($c = 0.5$, $CHCl_3$); ^{1}H NMR (300 MHz, $CDCl_3$): $\delta = 7.95$–7.85 (m, 2H), 7.74–7.65 (m, 2H), 7.64–7.52 (m, 4H), 7.46–7.40 (m, 1H), 7.34–7.24 (m, 5H), 7.21–7.17 (m, 2H), 6.29 (brs, 1H), 2.92–2.80 (m, 3H), 2.77–2.58 (m, 2H), 2.45–2.25 (m, 2H), 2.24–2.07 (m, 1H), 1.87–1.70 (m, 6H), 1.68–1.49 ppm (m, 2H); ^{13}C NMR (100 MHz, $CDCl_3$): $\delta = 137.8$, 133.3, 133.1, 132.7, 132.5, 131.8, 131.6, 131.5, 128.9, 128.6, 128.3, 128.3, 127.8, 127.6, 127.5, 127.4, 127.3, 125.9, 45.5, 29.3, 27.9, 22.7, 22.6, 22.5 ppm; ^{19}F NMR (282 MHz, $CDCl_3$): $\delta = -78.48$ ppm; ^{31}P NMR (121 MHz, $CDCl_3$): $\delta = -5.63$ ppm; IR (KBr): $\nu = 3444$ (b), 2932, 1440, 1289, 1198, 1095, 964, 945, 903, 818, 751, 614 cm^{-1}; ESI-MS: *m*/*z* (%): 738.6 (100) $[M-H]^-$.

Compound 35c: White foam; m.p. 155–159 °C; $[\alpha]_D^{20} = -235.8$ ($c = 0.5$, $CHCl_3$); ^{1}H NMR (300 MHz, $CDCl_3$): $\delta = 7.53$–7.40 (m, 4H), 7.35–7.10 (m, 8H), 4.33 (s, 1H), 2.86–2.74 (m, 3H), 2.71–2.51 (m, 3H), 2.36–2.19 (m, 2H), 1.83–1.67 (m, 6H), 1.62–1.47 ppm (m, 2H); ^{13}C NMR (100 MHz, $CDCl_3$): $\delta = 142.8$, 142.6, 137.9, 137.8, 136.7, 136.7, 135.9, 135.8, 131.7, 131.6, 131.3, 131.1, 129.9, 129.6, 128.2, 128.0, 127.4, 127.3, 127.2, 45.7, 45.7, 29.3, 29.2, 27.9, 22.6, 22.6, 22.5, 22.4 ppm; ^{19}F NMR (282 MHz, $CDCl_3$): $\delta = -78.43$ ppm; ^{31}P NMR (121 MHz, $CDCl_3$): $\delta =$

−4.48 ppm; IR (KBr): ν = 3443, 2933, 1448, 1292, 1200, 1096, 960, 887, 700, 605 cm^{-1}; ESI-MS: m/z (%): 638.5 (100) $[M-H]^-$.

Compound 35d: White foam; m.p. 250–254 °C; $[\alpha]_D^{20} = -263.4$ (c = 0.5, $CHCl_3$); ^{1}H NMR (300 MHz, $CDCl_3$): δ = 7.61–7.38 (m, 12H), 7.34–7.12 (m, 8H), 2.88–2.76 (m, 3H), 2.72–2.44 (m, 3H), 2.40–2.20 (m, 2H), 1.86–1.69 (m, 6H), 1.63–1.48 ppm (m, 2H); ^{13}C NMR (100 MHz, $CDCl_3$): δ = 140.8, 131.2, 131.2, 130.2, 129.9, 128.7, 128.7, 127.3, 127.2, 127.1, 127.1, 127.01, 127.00, 126.9, 126.6, 29.3, 29.3, 27.9, 22.6, 22.6, 22.5, 22.5 ppm; ^{19}F NMR (282 MHz, $CDCl_3$): δ = −78.20 ppm; ^{31}P NMR (121 MHz, $CDCl_3$): δ = −5.4 ppm; IR (KBr): ν = 3438 (b), 2932, 1489, 1448, 1428, 1293, 1198, 1095, 959, 888, 766, 698, 608 cm^{-1}; ESI-MS: m/z (%): 790.8 (100) $[M-H]^-$.

Compound 35e: White foam; m.p. 240–246 °C; $[\alpha]_D^{20} = -106.1$ (c = 0.5, $CHCl_3$); ^{1}H NMR (300 MHz, $CDCl_3$): δ = 8.81–8.40 (m, 4H), 8.11–7.01 (m, 16H), 4.86 (brs, 1H), 3.04–2.68 (m, 4H), 2.62–2.33 (m, 2H), 2.12–1.61 ppm (m, 10H); ^{13}C NMR (100 MHz, $CDCl_3$): δ = 132.5, 130.2, 130.1, 130.1, 130.0, 130.0, 129.7, 129.6, 129.6, 128.8, 126.7, 126.7, 126.6, 126.6, 126.6, 126.6, 126.6, 126.5, 126.5, 126.5, 126.4, 126.4, 126.4, 126.4, 126.4, 126.4, 126.4, 126.3, 126.3, 126.3, 126.1, 126.1, 122.5, 122.5, 122.0, 29.3, 29.3, 28.1, 22.7, 22.7, 22.6, 22.6, 22.6, 22.6, 22.5 ppm; ^{19}F NMR (282 MHz, $CDCl_3$): δ = −78.88 ppm; ^{31}P NMR (121 MHz, $CDCl_3$): δ = −3.4, −4.4 ppm; IR (KBr): ν = 3445 (b), 2930, 1624, 1450, 1422, 1301, 1194, 1087, 951, 888, 727, 617 cm^{-1}; ESI-MS: m/z (%): 838.6 (100) $[M-H]^-$.

Compound 35f: White foam; m.p. 188–192 °C; $[\alpha]_D^{20} = -134.9$ (c = 0.5, $CHCl_3$); ^{1}H NMR (300 MHz, $CDCl_3$): δ = 7.97 (m, 4H), 7.83 (m, 1H), 7.74 (m, 1H), 7.25 (brs, 2H), 2.94 (q, J = 6.6 Hz, 4H), 2.60–2.80 (m, 2H), 2.3–2.5 (m, 2H), 1.80–2.00 (m, 6H), 1.60–1.80 ppm (m, 2H); ^{13}C NMR (100 MHz, $CDCl_3$): δ = 140.7, 140.6, 140.3, 140.0, 138.0, 137.7, 137.6, 132.1, 131.9, 131.6, 131.5, 129.9, 129.5, 128.9, 126.6, 126.5, 125.0, 121.5, 121.4, 29.1, 29.1, 27.9, 22.1 ppm; ^{19}F NMR (282.2 MHz, $CDCl_3$): δ = −62.9, −63.0, −77.8, −79.0 ppm; ^{31}P NMR (121.4 MHz, $CDCl_3$): −7.3 ppm; IR (KBr): ν = 3392, 3281, 2943, 1389, 1375, 1279, 1188, 1136, 897, 682, 617 cm^{-1}; ESI-MS: m/z (%): 910.7 (100) $[M-H]^-$.

Compound 35g: White foam; m.p. 200–205 °C; $[\alpha]_D^{20} = -57.1$ (c = 0.5, $CHCl_3$); ^{1}H NMR (300 MHz, $CDCl_3$): δ = 6.70–7.10 (m, 6H), 5.2 (brs, 1H), 2.60–2.90 (m, 6H), 2.25–2.45 (m, 5H), 2.25 (m, 5H), 1.95–2.15 (m, 9H), 1.61–1.90 ppm (m, 9H); ^{13}C NMR (100 MHz, $CDCl_3$): δ = 143.1, 137.3, 137.2, 136.0, 132.5, 132.3, 130.2, 129.4, 128.9, 128.1, 127.8, 126.3, 126.1, 29.2, 27.8, 27.8, 22.6, 22.5, 21.3, 21.0, 20.8, 20.3, 20.0 ppm; ^{19}F NMR (282.2 MHz, $CDCl_3$): δ = −77.6, −79.6 ppm; ^{31}P NMR (121.4 MHz, $CDCl_3$): δ = 1.70, −6.75 ppm; IR (KBr): ν = 3444, 2928, 1451, 1287, 1198, 964, 882, 610 cm^{-1}; ESI-MS: m/z (%): 722.5 (100) $[M-H]^-$.

Compound 35h: White foam; m.p. 250–253 °C; $[\alpha]_D^{20} = -215{,}8$ (c = 0.5, $CHCl_3$); ^{1}H NMR (300 MHz, $CDCl_3$): δ = 7.40–7.50 (m, 4H), 7.22 (s, 1H), 7.17 (s, 1H), 6.94 (m, J = 8.7 Hz, 2H), 6.86 (m, J = 8.7 Hz, 2H), 4.40 (brs, 1H), 3.78 (s, 3H), 3.74 (s, 3H), 2.8–3.0 (m, 4H), 2.6–2.8 (m, 2H), 2.2–2.5 (m, 2H), 1.65–1.9 (m, 6H), 1.5–1.65 ppm (m, 2H); ^{13}C NMR (75.4 MHz, $CDCl_3$): δ = 159.4, 159.1, 142.2, 141.3, 137.9, 137.2, 136.6, 136.2, 131.6, 131.4, 131.0, 130.8, 130.6, 128.5, 128.2, 126.7, 126.5, 114.2, 113.5, 55.2, 55.1, 29.2, 27.7, 22.5 ppm; ^{19}F NMR (282.2 MHz, $CDCl_3$): δ = −77.4 ppm; ^{31}P NMR (121.4 MHz, $CDCl_3$): δ = −7.8 ppm; IR (KBr): ν = 3445, 2934, 1610, 1516, 1434, 1289, 1247, 1200, 959, 889, 833, 607, 571 cm^{-1}; ESI-MS: m/z (%): 698.6 (100) $[M-H]^-$.

Compound 35i: White foam; m.p. 194–198 °C; $[\alpha]_D^{20} = -214$ (c = 0.1, $CHCl_3$); ^{1}H NMR (400 MHz, $CDCl_3$): δ = 7.50 (d, J = 8.6 Hz, 2H), 7.38–7.44 (m, 4H), 7.32 (d, J = 8.2 Hz, 2H), 7.25 (s, 1H), 7.18 (s, 1H), 4.4 (b, 1H), 2.8–3.0 (m, 4H), 2.6–2.8 (m, 2H), 2.3–2.5 (m, 2H), 1.76–1.92 (m, 6H), 1.58–1.72 (m, 2H), 1.27 (s, 9H), 1.19 ppm (s, 9H); ^{13}C NMR (100 MHz, $CDCl_3$): δ = 150.2, 150.1, 137.8, 137.2, 136.3, 135.7, 133.3, 132.9, 131.6, 131.6, 131.4, 131.3, 131.0, 129.2, 129.0, 126.7, 125.2, 124.7, 45.6, 34.5, 34.4, 31.2, 31.2, 29.4, 29.3, 27.9, 27.8, 22.7, 22.7, 22.6, 22.5 ppm; ^{19}F NMR (376.3 MHz, $CDCl_3$): δ = −78.4 ppm; ^{31}P NMR (161.9 MHz, $CDCl_3$): δ = −6.0 ppm; IR (KBr): ν = 3437, 3019, 2962, 2866, 2664, 1648, 1517, 1433, 1388, 1286, 1200, 1160, 1099, 1064, 960, 892, 836, 758, 609 cm^{-1}; EI-MS: m/z (%): 751 (100) $[M]^+$, 680, (31), 360 (38), 86 (12).

Compound 35j: White foam; m.p. 216–220 °C; $[\alpha]_D^{20} = -149.6$ (c = 0.5, $CHCl_3$); ^{1}H NMR (300 MHz, $CDCl_3$): δ = 7.49–7.39 (m, 4H), 7.27–7.20 (m, 2H), 7.19–7.05 (m, 6H), 5.97 (brs. 1H), 2.88–2.70 (m, 2H), 2.70–2.47 (m, 4H), 2.33–2.16 (m, 2H), 1.82–1.63 (m, 6H), 1.60–1.40 ppm (m, 2H), ^{13}C NMR (100 MHz, $CDCl_3$): δ = 143.0, 142.9, 142.5, 142.3, 137.7, 137.7, 137.6, 137.6, 136.9, 136.9, 135.6, 135.6, 135.6, 135.6, 131.8, 131.8, 131.8, 131.7, 131.3, 131.2, 130.9, 130.9, 129.9, 129.6, 128.1, 127.9, 127.4, 127.4, 127.2, 127.1, 126.9, 126.9, 45.7, 29.3, 29.2, 27.9, 27.8, 22.7, 22.6, 22.6, 22.5 ppm; ^{19}F NMR (282 MHz, $CDCl_3$): δ = −80.87, −112.13, −121.37, −126.07 ppm; ^{31}P NMR (121 MHz, $CDCl_3$): δ = −4.43 ppm; IR (KBr): ν = 3445 (b), 2933, 1453, 1304, 1197, 1155, 1135, 958, 886, 699 cm^{-1}; ESI-MS: m/z (%): 788.6 (100) $[M-H]^-$.

Compound 35k: White foam; m.p. 119–123 °C; $[\alpha]_D^{20} = -139$ (c = 0.5, $CHCl_3$); ^{1}H NMR (300 MHz, $CDCl_3$): δ = 7.51–7.40 (m, 4H), 7.31–7.22 (m, 2H), 7.22–7.06 (m, 6H), 5.35 (brs, 1H), 2.91–2.72 (m, 2H), 2.72–2.50 (m, 4H), 2.37–2.17 (m, 2H), 1.85–1.65 (m, 6H), 1.64–1.41 ppm (m, 2H); ^{13}C NMR (75 MHz, $CDCl_3$): δ = 142.9, 142.8, 142.3, 142.2, 137.8, 137.8, 137.6, 137.6, 136.8, 136.8, 136.8, 135.8, 135.7, 135.7, 135.6, 131.8, 131.8, 131.3, 131.3, 131.1, 131.0, 129.9, 129.6, 128.2, 127.9, 127.3, 127.3, 127.3, 127.1, 126.8, 126.8, 45.6, 29.3, 29.2, 27.9, 22.7, 22.6, 22.5 ppm, ^{19}F NMR (282 MHz, $CDCl_3$): δ = −70.13, −71.90, −80.86, −111.76, −120.36, −121.80, −122.78, −126.16 ppm; ^{31}P NMR (121 MHz, $CDCl_3$): δ = −4.79 ppm; IR (KBr): ν = 2937, 1455, 1202, 1154, 960, 887, 700 cm^{-1}; ESI-MS: m/z (%): 988.8 (100) $[M-H]^-$.

Compound 35l: White foam; m.p. 158–161 °C; $[\alpha]_D^{20} = -218.2$ (c = 0.5, $CHCl_3$); ^{1}H NMR (300 MHz, $CDCl_3$): δ = 7.50–7.42 (m, 4H), 7.41–7.30 (m, 5H), 7.30–7.23 (m, 2H), 7.18 (s, 1H), 7.07–6.93 (m, 4H), 2.88–2.72 (m, 4H), 2.72–2.50 (m, 2H), 2.41–2.26 (m, 1H), 2.22–2.06 (m, 1H), 1.85–1.44 ppm (m, 8H); ^{13}C NMR (75 MHz, $CDCl_3$): δ = 138.3, 138.2, 137.7, 137.6, 136.5, 136.5, 136.4, 136.2, 136.0, 135.9, 131.8, 131.8, 131.7, 131.6, 131.5, 131.5, 131.5, 129.8, 129.4, 128.7, 127.9, 127.8, 127.7, 127.2, 125.7, 125.7, 29.2, 29.2, 27.9, 27.8, 22.6, 22.5, 22.4, 22.4 ppm; ^{19}F NMR (282 MHz, $CDCl_3$): δ = −63.28 ppm; ^{31}P NMR (121 MHz, $CDCl_3$): δ = −6.76 ppm; IR (KBr): ν = 2933, 1449, 1407, 1322, 1172, 1133, 1063, 943, 700, 598 cm^{-1}; ESI-MS: m/z (%): 714.6 (100) $[M-H]^-$.

Compound 35m: White foam; m.p. 141–144 °C; $[\alpha]_D^{20} = -264{,}7$ (c = 1.0, $CHCl_3$); ^{1}H NMR (300 MHz, $CDCl_3$): δ = 7.42 (s, 1H), 7.41 (s, 1H), 4.5 (brs, 1H), 2.7–2.9 (m, 4H), 2.45–2.6 (m, 2H), 2.15–2.3 (m, 2H), 1.7–1.85 (m, 6H), 1.45–1.65 ppm (m, 2H); ^{13}C NMR (75 MHz, $CDCl_3$): δ = 142.4, 142.2, 141.6, 141.5, 138.4, 138.4, 138.1, 138.1, 138.1, 138.0, 138.0, 137.9, 134.0, 133.9, 133.9, 133.9, 127.0, 126.9, 126.8, 126.7, 112.3, 112.2, 111.7, 111.6, 28.9, 28.8, 27.6, 27.6, 22.1, 22.0, 22.0, 21.9 ppm; ^{19}F NMR (282.2 MHz, $CDCl_3$): δ = −76.9, −78.9 ppm; ^{31}P NMR (121.4 MHz, $CDCl_3$): δ = −6.2 ppm; IR (KBr): ν = 3444, 2936, 1281, 1205, 1096, 961, 877, 612 cm^{-1}; ESI-MS: m/z (%): 642.2 (48) $[M-H]^-$, 644.2 (100) $[M-H]^-$, 646.2 (57) $[M-H]^-$.

Silyl protection of 32 to form 36b: Compound **32** (1 g, 2.2 mmol) and triphenylchlorosilane (2.4 g, 7.9 mmol) were dissolved in a 1:1 mixture of dry chloroform and DMF (40 mL) and heated to 90 °C. After 2 h, further triphenylchlorosilane (0.5 g) was added and the reaction mixture was stirred for 12 h at 90 °C under an argon atmosphere. The solution was cooled to RT, triturated with a saturated aqueous solution of $NaHCO_3$ (40 mL) and stirred for 30 min. The crude mixture was washed twice with dichloromethane. The organic layer was washed with brine, dried over Na_2SO_4, filtered and evaporated under vacuum. The crude product was purified by flash chromatography (hexane/dichloromethane 5:1) to yield **36b** as a white foam (1.91 g, 89%). ^{1}H NMR (250 MHz, $CDCl_3$): δ = 7.42–7.28 (m, 19H), 7.20–7.11 (m, 11H), 6.99 (s, 2H), 2.67–2.50 (m, 2H), 2.48–2.33 (m, 2H), 2.13–1.94 (m, 4H), 1.59–1.29 ppm (m, 8H); ^{13}C NMR (75 MHz, $CDCl_3$): δ = 147.4, 136.2, 135.4, 135.4, 134.9, 133.3, 132.4, 130.3, 129.5, 127.9, 127.4, 111.7, 28.9, 27.5, 22.7, 22.4 ppm; ESI-MS: m/z (%): 986.4 (6) $[M+NH_4]^+$.

Rearrangement of 36b to form 37b: The silyl-protected BINOL **36b** (1.7 g, 1.8 mmol) was dissolved in THF (30 mL) and cooled to 0 °C. Under an argon atmosphere, a 1.5 M *t*BuLi solution in THF (3.7 mL, 5.6 mmol, 3.2 equiv) was added within 5 min. The ice bath was removed and the solution was stirred for 45 min at RT. The reaction mixture was quenched with a saturated aqueous solution of $NaHCO_3$ and washed twice with dichloromethane. The organic layers were combined, dried over Na_2SO_4, filtered and evaporated under vacuum to yield **37b** as white foam (1.4 g, 99%). The crude product was directly used in the final

phosphoramidation step. ^{1}H NMR (250 MHz, $CDCl_3$): δ = 7.75–7.59 (m, 12H), 7.51–7.36 (m, 18H), 7.00 (s, 2H), 4.94 (s, 2H), 2.71–2.59 (m, 4H), 2.48–2.34 (m, 4H), 1.83–1.71 ppm (m, 8H); ^{13}C NMR (75 MHz, $CDCl_3$): δ = 156.2, 140.1, 136.3, 134.7, 130.1, 129.4, 127.8, 118.9, 117.2, 34.7, 31.7, 29.2, 27.5, 26.9, 25.4, 22.7, 20.8 ppm; ESI-MS: *m*/*z* (%): 810.0 (100) $[M-H]^-$.

Compound 38a: White foam; m.p. 130–133 °C; $[\alpha]_D^{20} = -159.8$ (*c* = 0.5, $CHCl_3$); ^{1}H NMR (300 MHz, $CDCl_3$): δ = 7.59–7.46 (m, 4H), 7.39–7.05 (m, 18H), 4.80 (bs, 1H), 2.77–2.63 (m, 2H), 2.64–2.40 (m, 4H), 2.24–2.04 (m, 2H), 1.76–1.44 (m, 8H), 0.90 (s, 3H), 0.87 (s, 3H); ^{13}C NMR (100 MHz, $CDCl_3$): δ = 140.4, 139.3, 137.9, 136.2, 135.8, 135.7, 135.7, 135.6, 135.6, 135.5, 135.4, 135.2, 134.9, 129.9, 129.9, 129.3, 129.1, 129.0, 128.5, 128.4, 128.3, 128.2, 127.8, 127.6, 125.3, 29.1, 27.9, 27.8, 22.5, 22.4, 22.3; ^{19}F NMR (282.2 MHz, $CDCl_3$): δ = −77.3; ^{31}P NMR (121.4 MHz, $CDCl_3$): δ = −9.2; IR (neat): ν = 3445, 2934, 1428, 1282, 1195, 1110, 1080, 962, 789, 735, 611 cm^{-1}; ESI-MS: *m*/*z* (%): 878.8 (100) $[M-H]^-$.

Compound 38b: White foam; m.p. 160–163 °C; $[\alpha]_D^{20} = -159.0$ (*c* = 0.5, $CHCl_3$); ^{1}H NMR (300 MHz, $CDCl_3$): δ = 7.57–7.50 (m, 6H), 7.48–7.40 (m, 6H), 7.35–7.16 (m, 19H), 6.96 (s, 1H), 3.19 (bs, 1H), 2.73–2.64 (m, 2H), 2.63–2.46 (m, 4H), 2.35–2.11 (m, 2H), 1.82–1.47 ppm (m, 8H); ^{13}C NMR (100 MHz, $CDCl_3$): δ = 150.5, 150.5, 141.6, 141.5, 140.8, 140.7, 140.2, 140.1, 139.4, 139.4, 136.8, 136.5, 136.4, 136.4, 135.6, 135.5, 135.4, 135.3, 133.5, 133.2, 129.9, 129.4, 128.2, 127.6, 127.6, 126.5, 126.4, 125.7, 122.3, 122.8, 121.5, 121.4, 29.1, 28.0, 27.9, 22.6, 22.5, 22.5, 22.4 ppm; ^{19}F NMR (282.2 MHz, $CDCl_3$): δ = −77.9 ppm; ^{31}P NMR (121.4 MHz, $CDCl_3$): δ = −10.8 ppm; IR (KBr): ν = 3445, 2933, 1428, 1302, 1197, 1107, 975, 912, 701, 612 cm^{-1}; ESI-MS: *m*/*z* (%): 1003.2 (26) $[M-H]^-$.

Acknowledgements

We acknowledge financial support from DFG (Priority program Organocatalysis) and the Fonds der Chemischen Industrie for stipends given to B.J.N. and R.M.K.

[1] a) D. Uraguchi, M. Terada, *J. Am. Chem. Soc.* **2004**, *126*, 5356–5357; b) M. Terada, D. Uraguchi, K. Sorimachi, H. Shimizu, PCT Int. Appl. WO 2005070875, **2005**; c) T. Akiyama, J. Itoh, K. Yokota, K. Fuchibe, *Angew. Chem.* **2004**, *116*, 1592–1594; *Angew. Chem. Int. Ed.* **2004**, *43*, 1566–1568; d) T. Akiyama, PCT Int. Appl. WO 200409675, **2004**; for reviews on chiral phosphoric acids, see: e) M. Terada, *Chem. Commun.* **2008**, 4097–4112; f) M. Terada, *Synthesis* **2010**, 1929–1982.

[2] For reviews on Brønsted acid catalysis, see: a) T. Akiyama, *Chem. Rev.* **2007**, *107*, 5744–5758; b) T. Akiyama, J. Itoh, K. Fuchibe, *Adv. Synth. Catal.* **2006**, *348*, 999–1010; c) M. S. Taylor, E. N. Jacobsen, *Angew. Chem.* **2006**, *118*, 1550–1573; *Angew. Chem. Int. Ed.* **2006**, *45*, 1520–1543; d) A. G. Doyle, E. N. Jacobsen, *Chem. Rev.* **2007**, *107*, 5713–5743; e) H. Yamamoto, N. Payette, in *Hydrogen Bonding in Organic Synthesis* (Ed.: P. M. Pihko), Wiley-VCH, Weinheim, **2009**, pp. 73–140.

[3] For examples of carbonyl activation, see: a) S. Xu, Z. Wang, X. Zhang, K. Ding, *Angew. Chem.* **2008**, *120*, 2882–2885; *Angew. Chem. Int. Ed.* **2008**, *47*, 2840–2843; b) M. Terada, K. Soga, N. Momiyama, *Angew. Chem.* **2008**, *120*, 4190–4193; *Angew. Chem. Int. Ed.* **2008**, *47*, 4122–4125; c) T. Akiyama, T. Katoh, K. Mori, *Angew. Chem.* **2009**, *121*, 4290–4292; *Angew. Chem. Int. Ed.* **2009**, *48*, 4226–4228; d) K. Mori, T. Katoh, T. Suzuki, T. Noji, M. Yamanaka, T. Akiyama, *Angew. Chem.* **2009**, *121*, 9832–9834; *Angew. Chem. Int. Ed.* **2009**, *48*, 9652–9654; e) W. Kashikura, J. Itoh, K. Mori, T. Akiyama, *Chem. Asian J.* **2010**, *5*, 470–472; f) Q. Gu, Z.-Q. Rong, C. Zheng, S.-L. You, *J. Am. Chem. Soc.* **2010**, *132*, 4056–4057.

[4] The pK_a of diethylphosphate is 1.3.

[5] a) P. Burk, I. A. Koppel, I. Koppel, L. M. Yagupolskii, R. W. Taft, *J. Comput. Chem.* **1996**, *17*, 30–41; b) I. Leito, I. Kaljurand, I. A. Koppel, L. M. Yagupolskii, V. M. Vlasov, *J. Org. Chem.* **1998**, *63*, 7868–7874; c) I. A. Koppel, P. Burk, I. Koppel, I. Leito, T. Sonoda, M. Mishima, *J. Am. Chem. Soc.* **2000**, *122*, 5114–5124; d) I. A. Koppel, J. Koppel, I. Leito, I. Koppel, M. Mishima, L. M. Yagupolskii, *J. Chem. Soc. Perkin Trans. 2* **2001**, 229–232; e) L. M. Yagupolskii, V. N. Petrik, N. V. Kondratenko, L. Soovali, I. Kaljurand, I. Leito, I. A. Koppel, *J. Chem. Soc. Perkin Trans. 2* **2002**, 1950–1955.

[6] For determination of the pK_a of amidated phosphoric acid, see: B. T. Burlingham, T. S. Widlanski, *J. Org. Chem.* **2001**, *66*, 7561–7567.

[7] D. Nakashima, H. Yamamoto, *J. Am. Chem. Soc.* **2006**, *128*, 9626–9627.

[8] P. Jiao, D. Nakashima, H. Yamamoto, *Angew. Chem.* **2008**, *120*, 2445–2447; *Angew. Chem. Int. Ed.* **2008**, *47*, 2411–2413.

[9] a) M. Rueping, W. Ieawsuwan, A. P. Antonchick, B. J. Nachtsheim, *Angew. Chem.* **2007**, *119*, 2143–2146; *Angew. Chem. Int. Ed.* **2007**, *46*, 2097–2100; b) M. Rueping, W. Ieawsuwan, *Adv. Synth. Catal.* **2009**, *351*, 78–84.

[10] M. Rueping, B. J. Nachtsheim, S. A. Moreth, M. Bolte, *Angew. Chem.* **2008**, *120*, 603–606; *Angew. Chem. Int. Ed.* **2008**, *47*, 593–596.

[11] M. Rueping, T. Theissmann, A. Kuenkel, R. M. Koenigs, *Angew. Chem.* **2008**, *120*, 6903–6906; *Angew. Chem. Int. Ed.* **2008**, *47*, 6798–6801.

[12] M. Rueping, M.-Y. Lin, *Chem. Eur. J.* **2010**, *16*, 4169–4172.

[13] M. Rueping, B. J. Nachtsheim, *Synlett* **2010**, 119–122.

[14] For further examples of *N*-triflylphosphoramides in enantioselective catalysis, see: a) D. Enders, A. Narine, F. Toulgoat, T. Bisschops, *Angew. Chem.* **2008**, *120*, 5744–5748; *Angew. Chem. Int. Ed.* **2008**, *47*, 5661–5665; b) M. Zeng, Q. Kang, Q.-L. He, S.-L. You, *Adv. Synth. Catal.* **2008**, *350*, 2169–2173; c) S. Lee, S. Kim, *Tetrahedron Lett.* **2009**, *50*, 3345–3348; for the application of *N*-triflylthiophosphoramides, see: d) C. H. Cheon, H. Yamamoto, *J. Am. Chem. Soc.* **2008**, *130*, 9246–9247; e) C. H. Cheon, H. Yamamoto, *Org. Lett.* **2010**, *12*, 2476–2479.

[15] a) P. J. Cox, W. Wang, V. Snieckus, *Tetrahedron Lett.* **1992**, *33*, 2253–2256; b) K. B. Simonsen, K. V. Gothelf, K. A. Jorgensen, *J. Org. Chem.* **1998**, *63*, 7536–7538; c) S. S. Zhu, D. R. Cefalo, D. S. La, J. Y. Jamieson, W. M. Davis, A. H. Hoveyda, R. R. Schrock, *J. Am. Chem. Soc.* **1999**, *121*, 8251–8259; d) Y. Chen, S. Yekta, A. K. Yudin, *Chem. Rev.* **2003**, *103*, 3155–3211.

[16] For a representative synthesis of 3,3′-arylated BINOLs **29**, see: M. Rueping, E. Sugiono, C. Azap, T. Theissmann in *Catalysts for Fine Chemical Synthesis, Vol. 5* (Eds.: S. M. Roberts, J. Whittall), Wiley, Chichester, **2007**, pp. 161–181. The synthesis of **29f** has been described as part of the synthesis of the corresponding phosphoric acid derivative.

[17] For the bromination of H_8-BINOL, see: a) D. J. Cram, R. C. Helgeson, S. C. Peacock, L. J. Kaplan, L. A. Domeier, P. Moreau, K. Koga, J. M. Mayer, Y. Chao, M. G. Siegel, D. H. Hoffman, G. D. Y. Sogah, *J. Org. Chem.* **1978**, *43*, 1930–1946; b) N. T. McDougal, S. E. Schaus, *J. Am. Chem. Soc.* **2003**, *125*, 12094–12095.

[18] For the direct Suzuki coupling of H_8-BINOL, see: M. Bartoszek, M. Beller, J. Deutsch, M. Klawonn, A. Kockritz, N. Nemati, A. Pews-Davtyan, *Tetrahedron* **2008**, *64*, 1316–1322.

[19] For the synthesis of silylated H_8-BINOL derivatives, see: a) N. V. Sewgobind, M. J. Wanner, S. Ingemann, R. de Gelder, J. H. van Maarseveen, H. Hiemstra, *J. Org. Chem.* **2008**, *73*, 6405–6408; for the synthesis of silylated BINOL derivatives, see: b) K. Maruoka, T. Itoh, Y. Araki, T. Shirasaka, H. Yamamoto, *Bull. Chem. Soc. Jpn.* **1988**, *61*, 2975–2976; c) R. I. Storer, D. E. Carrera, Y. Ni, D. W. C. MacMillan, *J. Am. Chem. Soc.* **2006**, *128*, 84–86.

[20] *Holleman-Wiberg's Inorganic Chemistry* (Ed.: N. Wiberg), Academic Press, New York, **2001**.

[21] For recent reviews, see: a) T. T.-L. Au-Yeung, S.-S. Chan, A. S. C. Chan, *Adv. Synth. Catal.* **2003**, *345*, 537–555; b) Y.-M. Li, M. Yan, A. S. C. Chan, in *Phosphorus Ligands in Asymmetric Catalysis* (Ed.: A. Boerner), Wiley-VCH, Weinheim, **2008**, pp. 284–306.

[22] a) Phosphoric acids and the corresponding calcium salts were found to catalyse Mannich reaction between aldimines and various 1,3-dicarbonyl compounds, leading to products with opposite stereochem-

istry at the chiral amine centre: M. Hatano, K. Moriyama, T. Maki, K. Ishihara, *Angew. Chem.* **2010**, *122*, 3911–3914; *Angew. Chem. Int. Ed.* **2010**, *49*, 3823–3826; b) for a study describing the synthesis of the commercially available TRIP catalyst and practical ways to distinguish between the metal contaminated and the free acid, see: M. Klussmann, L. Ratjen, S. Hoffmann, V. Wakchaure, R. Goddard, B. List, *Synlett* DOI: 10.1055/s-0030-1258505.

Received: May 24, 2010
Published online: October 4, 2010

